Heat Transfer Through Post-Frame Building Walls

Andrew J. Holstein, PhD, and David R. Bohnhoff, PhD, PE

Introduction

A building's thermal envelope consists of all the components separating the interior conditioned space from its surroundings, thereby controlling the flow of heat. The flow of heat through a thermal envelope is a complex process that involves multiple modes of heat transfer (i.e., simultaneous conduction, convection, and radiation) and the interaction of material geometries and properties.

Heat Transfer in Post-Frame Buildings

Since its inception in the first half of the twentieth century, the post-frame structural system has gained a well-deserved reputation for structural efficiency, likely leading to its prevalence in the agricultural industry, where economy is paramount. The same large bay spacing that leads to reduced material usage also reduces the number of thermal breaks present in a wall, thereby increasing the effectiveness of a building's thermal envelope. Large structural posts typical of post-frame buildings lead to thick walls that offer many options for insulation. Commonly, at least some portion of the wall cavity is left uninsulated and contains either continuous or discontinuous air voids.

When evaluated using simplified methods, air voids are often assumed to be largely composed of still air, and therefore significant thermal resistances are attributed to them. Studies have shown, however, that the air in air voids is rarely still and that substantial heat transfer may occur via natural convection and radiation.

Predicting Heat Transfer

The simplest method of determining heat transfer in a thermal envelope is the use of one-dimensional heat flow equations such as the parallel path and isothermal plane methods suggested by ASHRAE (2017). These equations allow a designer to use basic resistance theory to sum thermal envelope components in either series or parallel to yield a resulting resistance value for the wall as a whole. Although these methods focus primarily on conduction heat transfer, ASHRAE suggests coefficients for estimating the contribution to heat transfer by radiation and natural convection across plane airspaces. However, these coefficients must be used with care because research has shown that simple formulae cannot be used to sum independent conduction, convection, and radiation heat flows.

A more accurate method for determining the performance of a thermal envelope incorporating conjugate heat transfer is through experimental evaluation of a large-scale envelope sample. Care must be taken to ensure that the envelope sample is constructed in a manner representative of field installation and that the negative effects of flanking loss and lateral conductance are minimized or accounted for.

Experimental Determination of Heat Transfer

Thermal performance may be determined experimentally through the use of an apparatus called a rotatable guarded hot box (RGHB). The main component of an RGHB (**Figure 1**) is its meter chamber, a five-sided insulated box that is applied to the warm side of a test specimen. Air inside the meter chamber is heated to a steady-state temperature, and further energy input is monitored. Conducting an energy balance for the meter chamber demonstrates that energy input must equal the energy leaving the meter chamber through either the five sides of the chamber or the test specimen. To isolate the energy flow through the test specimen, the meter chamber is placed inside another chamber maintained at the same steady-state temperature. Because there is no temperature differential across the five meter chamber walls, there is no heat flux and the meter chamber is "guarded" from heat loss; thus the outside chamber is referred to as the *guard chamber*. To test specimens over a greater temperature gradient, a climate chamber, which can be cooled and maintained at a lower steady-state temperature, is attached to the other side of the test specimen. So that samples may be tested at multiple orientations, the entire apparatus is mounted on a steel frame that allows it to rotate 360 degrees.

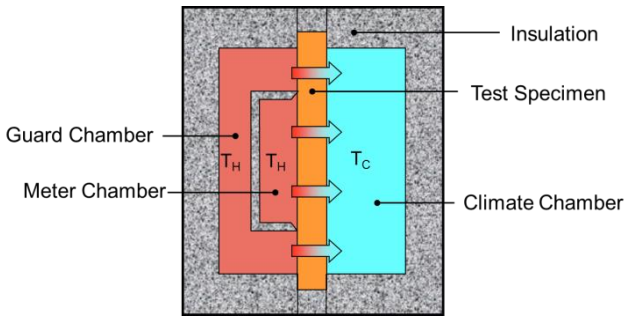

Figure 1. Schematic of a typical rotatable guarded hot box

An RGHB was developed at the University of Wisconsin–Madison (UW) to aid in evaluating the thermal performance of envelopes containing continuous or discontinuous air voids (Holstein & Bohnhoff, 2015; Holstein, 2017). The metering area of the UW RGHB is 8 feet high by 10 feet wide and accepts thermal envelope samples up to 12 inches thick. Energy is supplied to the meter chamber at a constant rate, and the energy balance used to determine thermal resistance is evaluated when the sample comes to temperature equilibrium, generally after approximately 72 hours. Samples may be evaluated over varying mean temperatures by altering the rate of energy supplied to the meter chamber.

Thermal Envelope Designs

Five thermal envelopes, detailed in the following sections, were evaluated for thermal performance using the UW RGHB. All five envelope designs consisted of a central I-shaped mechanically laminated wood post (**Figure 2**). The flanges of the post were nominal 2x6 dimensional lumber, and the web was constructed of nominal 2x6 laminated strand lumber (LSL). The warm surface of all designs was sheathed in 0.63-inch type X gypsum wall board secured with 1.63-inch drywall screws at an 8-inch perimeter spacing and 16-inch field spacing. All joints were sealed with paper tape and all-purpose joint compound. Gypsum was chosen for the warm surface because it simplifies meter chamber sealing for greater repeatability and represents a wall variation that could be expected in the industry, where fire resistance is desired. The cold surface of all designs was sheathed in 29-gauge steel ribbed panels secured with a 1-inch siding screw at each major rib, which were 9 inches on-center.

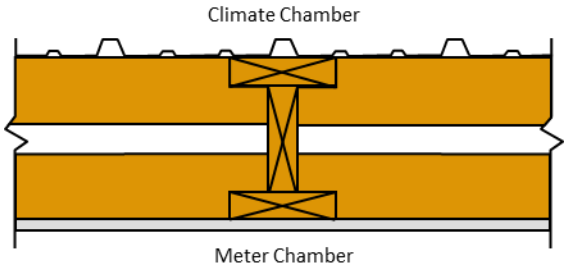

Figure 2. Typical plan view at center of the test wall (offset, inset nominal 2x4 notched girts shown)

Uninsulated Continuous Cavity Envelope

The uninsulated continuous (UC) cavity envelope consisted of offset, inset nominal 2x4 notched girts spaced 24 inches on center (**Figure 3a)**. Girts placed against the gypsum wall board were fabricated from LSL to ensure straight and consistent interfaces with the gypsum.

Insulated Continuous Cavity Envelope
The insulated continuous (IC) cavity envelope was proposed by Holstein and colleagues (2018) and varied from the UC cavity envelope only in the addition of a serpentine blanket of unfaced fiberglass insulation with a total thermal resistance of 19 hr-ft^2-°F/Btu (**Figure 3b**). (Additional details on the envelope may be found in Holstein et al., 2018.)

Uninsulated Discontinuous Cavity Envelope
The uninsulated discontinuous (UD) cavity envelope consisted of inset 1.5 x 8.5-inch double-notched LSL girts spaced 24 inches on center (**Figure 3c**). To prevent the transfer of air between discontinuous cavities, foam closure strips were installed between the girts and steel ribbed panels, and the remaining girt perimeter was sealed with silicone sealant.

Insulated Discontinuous Cavity Envelope
The insulated discontinuous (ID) cavity envelope varied from the UD envelope only in the addition of 5.5-inch-thick batts of unfaced fiberglass insulation with a total thermal resistance of 19 hr-ft^2-°F/Btu (**Figure 3d**). Fiberglass batts were carefully fit to the air voids to reduce air infiltration between the insulation and girts.

Radiant Barrier Discontinuous Cavity Envelope
The radiant barrier discontinuous (RD) cavity envelope varied from the UD envelope only in the removal of the foam closure strips and addition of a layer of 0.38-inch double-bubble radiant barrier insulation beneath the steel ribbed panels on the cold side of the air cavities (**Figure 3e**). Seams in the radiant barrier insulation were sealed with foil tape.

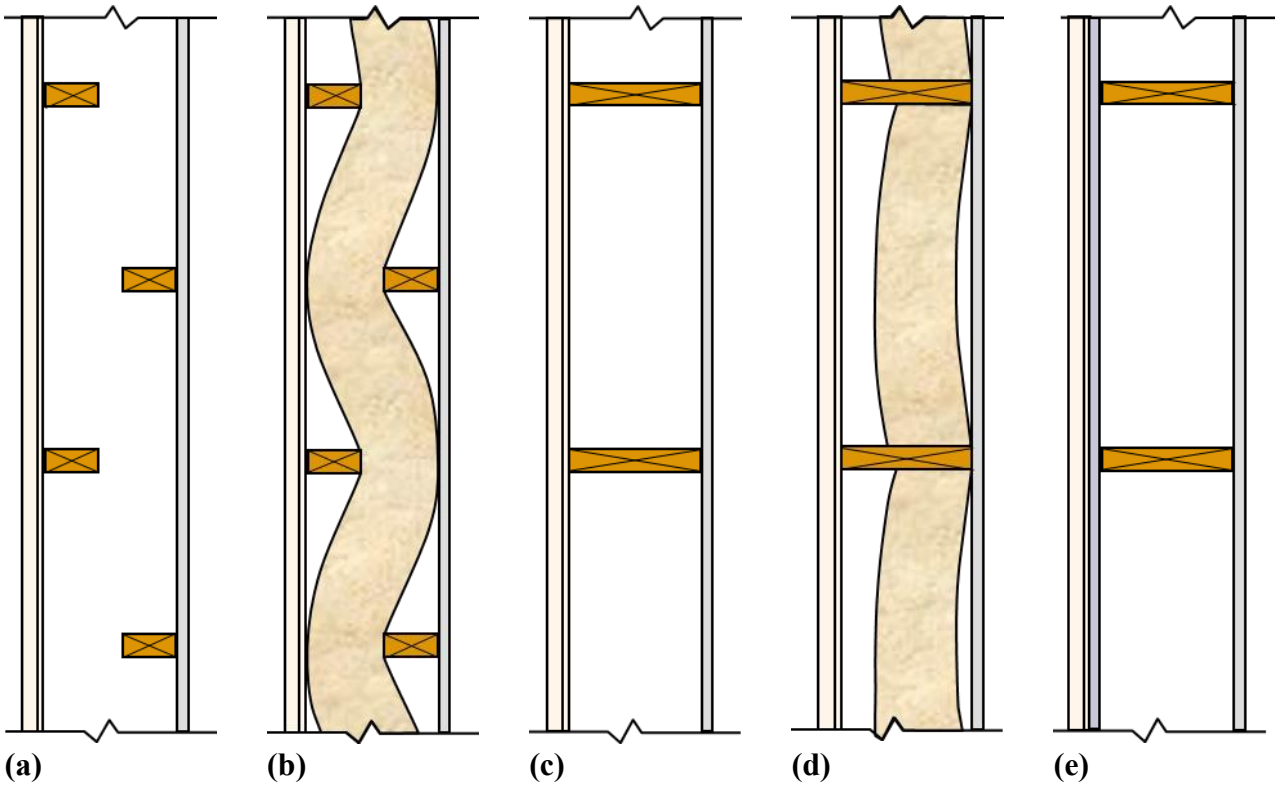

Figure 3. Cross-section view of (a) UC cavity envelope, (b) IC cavity envelope, (c) UD cavity envelope, (d) ID cavity envelope, and (e) RD cavity envelope

Test Procedures
Each envelope design was evaluated at a range of mean sample temperatures and tested in two orientations. More specifically, each specimen was oriented vertically to force net heat transfer in the

horizontal direction, and each specimen was oriented horizontally with the hot chamber on top to force net heat transfer downward. The final design (RD) was also tested in a horizontal orientation with the hot chamber on the bottom to force net heat transfer upward. In the remainder of this article, testing may be referred to by the direction of net heat transfer for brevity. For example, a test with the sample oriented horizontally to drive net heat transfer downward may simply be referred to as a downward test.

Although the evaluated envelope designs may not directly apply to typical roof or ceiling assemblies, forcing heat flow in a downward direction mimics the heat transfer in a low-slope roof during summer conditions where the conditioned space is maintained at a cooler temperature than its surroundings.

Results and Discussion

Plots of the thermal resistance of envelopes IC and ID are presented in **Figure 4**. Plots of the thermal resistance of envelopes UC and UD are presented in **Figure 5**. Plots of the thermal resistance of envelope RD are presented in **Figure 6**. Linear regressions were used to generate comparisons between the test groups.

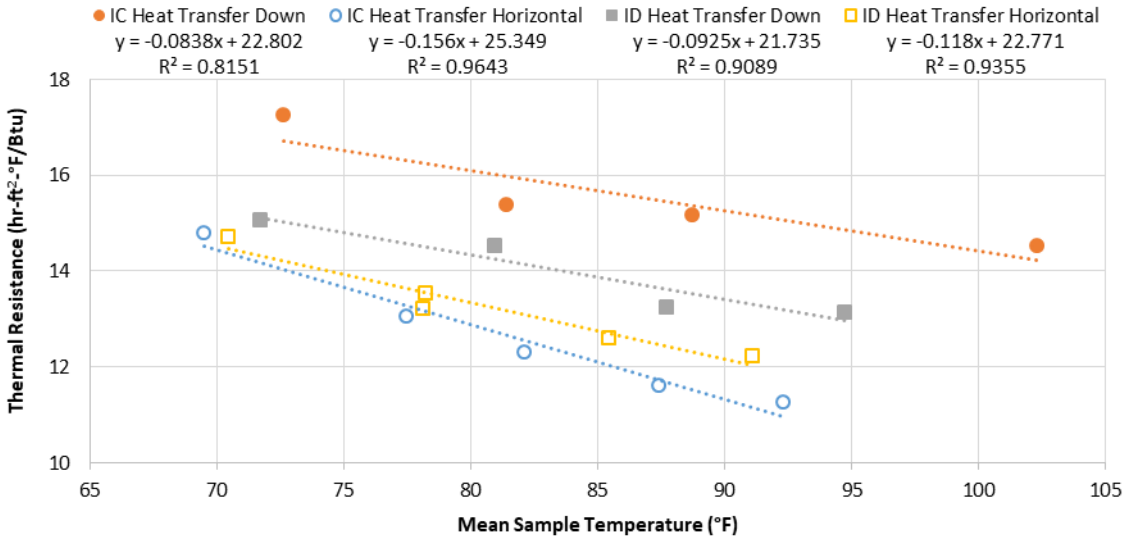

Figure 4. Plot of insulated envelope assemblies (IC and ID) depicting effect of mean sample temperature, girt design, and heat transfer orientation

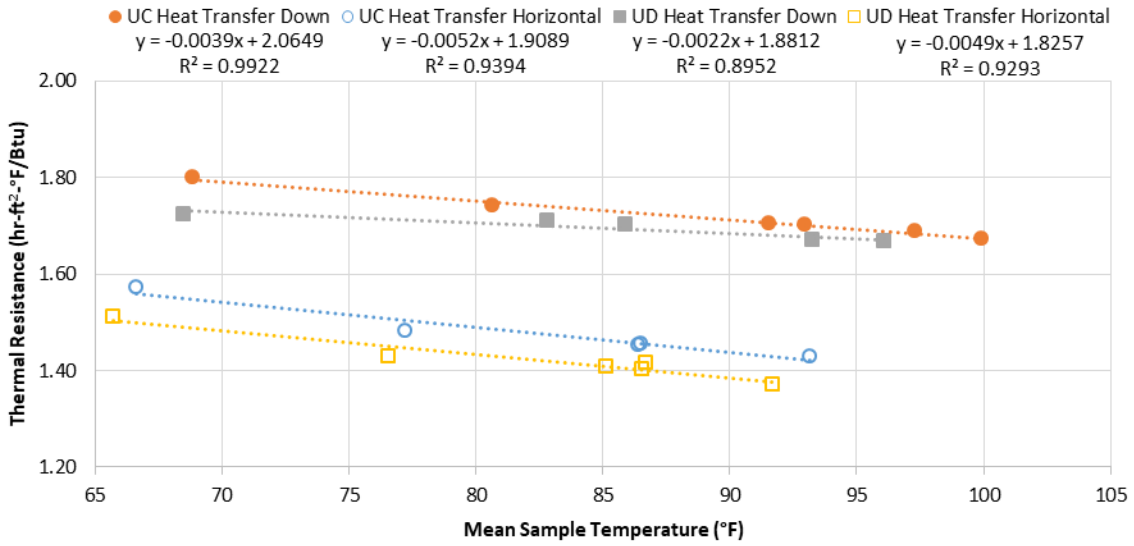

Figure 5. Plot of uninsulated envelope assemblies (UC and UD) depicting effect of mean sample temperature, girt design, and heat transfer orientation

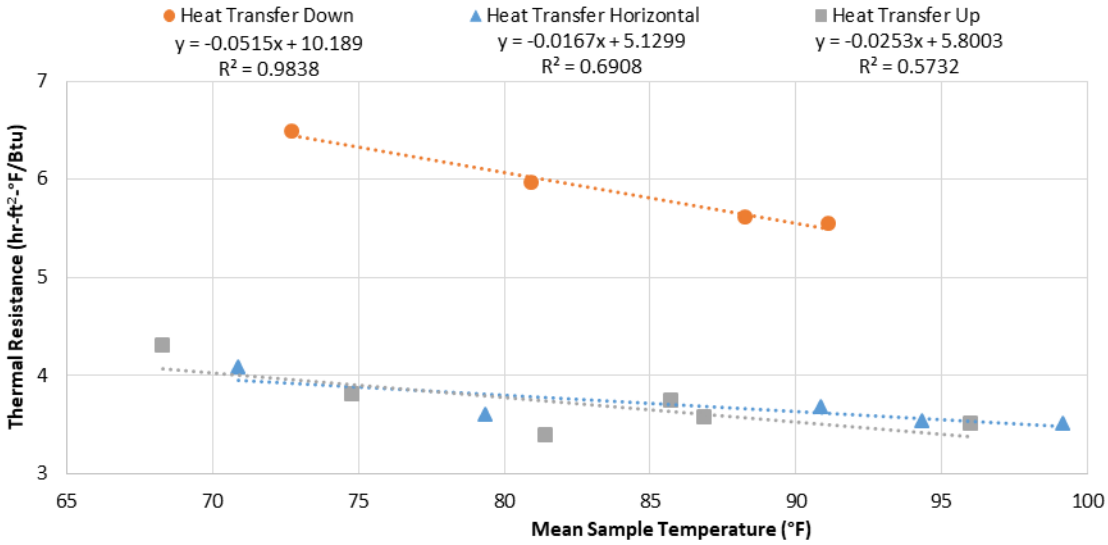

Figure 6. Plot of radiant barrier (RD) envelope depicting effect of mean sample temperature and heat transfer orientation

Table 1 contains a comparison of ASHRAE-predicted and experimentally determined effective thermal resistance values for all five envelope designs. Predicted values were calculated using the parallel path method and incorporate plane airspace resistances listed in Table 3 of Chapter 25 of the *ASHRAE Handbook—Fundamentals* (ASHRAE, 2017). The handbook provides plane airspace resistance values only for airspaces of 0.5, 0.75, 1.5, and 3.5 inches with "moderate" extrapolation allowed. The largest airspaces contained in envelopes UC and UD are 8.5 inches thick. Resistance values were extrapolated to a maximum 5.5-inch space for specimens with net heat transfer occurring horizontally because natural convection will begin to reduce thermal resistance in wider spaces. For predictions of downward heat transfer, resistance values were extrapolated to the full 8.5-inch space because natural convection is virtually eliminated within these airspaces and radiation is unaffected by the airspace thickness. Surface emissivity values were assumed to be 0.90 for all envelope materials with the exception of the double-bubble radiant barrier insulation, which was assumed to be 0.20 per

the recommendations of the 2017 *ASHRAE Handbook—Fundamentals*. The thermal conductivity of all lumber was assumed to be 0.82 Btu-in/hr-ft^2-°F, based on the average value tabulated for Spruce-Pine-Fir in the *ASHRAE Handbook—Fundamentals*.

Table 1. Comparison of Predicted and Experimentally Determined Effective Thermal Resistances

	Effective thermal resistance at 90°F mean sample temperature for downward heat transfer (hr-ft^2-°F/Btu)			Effective thermal resistance at 90°F mean sample temperature for horizontal heat transfer (hr-ft^2-°F/Btu)		
Envelope	Experimentally determined	ASHRAE predicted	ASHRAE Overprediction	Experimentally determined	ASHRAE predicted	ASHRAE Overprediction
UC	1.71	1.88	10%	1.44	1.54[a]	7%
UD	1.68	1.82	8%	1.38	1.48[a]	7%
IC	15.3	16.9	11%	11.3	16.8	49%
ID	13.4	16.0	19%	12.2	15.9	31%
RD	5.55	5.84	5%	3.63	2.87[a]	-21%

[a]The maximum 5.5-inch plane airspace used for calculation is less than experimental airspace.

Orientation Effects

Direction of net heat transfer had a substantial effect on effective thermal resistance. When specimens were rotated to drive heat transfer downward instead of horizontally, natural convection was virtually eliminated as a heat transfer mechanism, thereby increasing effective thermal resistance. On average, insulated samples (IC and ID) exhibited an effective thermal resistance to downward heat transfer that was 18% greater than that for horizontally driven heat transfer. The effect was especially pronounced in the IC design, where effective thermal resistance increased 28% with the change in heat transfer direction. Compared to envelope ID, envelope IC had a 13% greater effective thermal resistance value for downward heat transfer, which can be attributed to the offset girts of envelope IC providing a less direct path for thermal conduction.

The effect of orientation on uninsulated samples was similar, with the average effective thermal resistance value for design UC increasing 19% and that for design UD increasing 20% when heat transfer was directed downward instead of horizontally. Once again, envelope UC had greater average thermal resistance values than envelope UD; however, without insulation, radiant heat transfer was a larger component of total heat transfer, and the offset girts were less helpful, resulting in an increase of only 3%.

The design of envelope RD (with a wide airspace through which radiant heat transfer was reduced with reflective insulation) was associated with an especially large orientation effect. When heat flow was forced downward, heat transfer was largely restricted to conduction, and the design exhibited a 60% greater effective thermal resistance compared to an upward orientation and a 59% greater resistance compared to tests with heat flow directed horizontally. These results would also imply that *horizontal* heat transfer associated with convection in an airspace 8.5 inches wide and 22.5 inches high is roughly equal to *upward* heat transfer associated with convection in an airspace 22.5 inches wide and 8.5 inches high.

Temperature Effects

The thermal performance of tested designs was negatively affected by mean sample temperature, especially for horizontal heat transfer. On average, insulated tests (IC and ID) in which heat transfer was directed downward exhibited a 15% loss in effective thermal resistance between 68°F and 95°F, and tests in which heat transfer was directed horizontally exhibited a 25% loss over the same range. This is likely due to increases (with temperature) in the rate of natural convection. The temperature effects were less pronounced in uninsulated specimens, averaging a 5% reduction in effective thermal

resistance from 68°F to 95°F for downward heat flow and a 9% reduction in thermal resistance for tests with horizontal heat flow. As mean temperature was increased from 68°F to 95°F, the effective thermal resistance for envelope RD decreased 21%, 17%, and 11% for heat transfer directed downward, upward, and horizontally, respectively. The 2017 *ASHRAE Handbook— Fundamentals* estimates that the effective thermal resistance of the airspaces in envelope RD would decrease 15% when mean sample temperature increased from 68°F to 95°F.

Girt Configuration Effects

When conduction is expected to be a primary component of heat transfer, it is best to use the offset girt design of the UC and IC envelopes because it reduces the short circuiting of thermal energy through the specimen. Conversely, when natural convection is expected to be a primary component of heat transfer, it is best to use the full-width girt design of the UD and ID envelopes because they reduce the size and continuity of airspaces. Finally, the reflective surface of the RD envelope is best used when radiation is expected to be a primary component of heat transfer.

One-Dimensional Predictions

It is important to note that the tested envelopes generally failed to achieve the thermal resistance values predicted with the use of simple one-dimensional heat transfer equations. Predicted resistance values were on average 8% greater for uninsulated envelope designs (UC and UD) and 27% greater for insulated designs (IC and ID). The effective thermal resistance of IC for horizontally driven heat transfer was overpredicted by 49%.

The thermal resistance of envelope RD to downward heat flow was overpredicted by 5%, and its resistance to horizontal heat flow was underpredicted by 21%. This underprediction may be due to the conservative estimation of the double-bubble radiant barrier insulation's emissivity at 0.20. Although these one-dimensional correlations are derived from experiments that considered conjugate heat transfer, they do not always fully capture the complex nature of multimode, three-dimensional heat transfer in building envelopes.

Insulation Considerations

Some of the reduction in thermal performance exhibited in this study may be attributed to inaccuracies in the installation of insulation products. During installation of the unfaced fiberglass insulation in envelope IC, great care was taken, and yet the insulation was unable to achieve the desired serpentine geometry. This geometry was key to the enhanced thermal performance predicted by numerical modeling, and the installation discrepancies resulted in a reduced benefit over the ID envelope, exhibiting only 4%-higher thermal resistances on average.

Although the nominal thermal resistance of the double-bubble radiant barrier insulation was only 3.7 hr-ft^2-°F/Btu, approximately 20% of the unfaced fiberglass blanket nominal resistance of 19 hr-ft^2-°F/Btu, envelope RD achieved a thermal resistance equivalent to 42% of the thermal resistance of envelope ID when tested downward and 29% of the ID resistance when tested with heat transfer occurring horizontally. Nominal resistance values alone may not adequately inform decisions when one is comparing thermal envelope designs based on the complex interactions that insulation materials have with their surroundings.

Summary and Conclusions

Heat transfer through composite thermal envelopes containing continuous and discontinuous air voids is a complex phenomenon that is difficult to predict using one-dimensional equations. General trends, such as increased thermal resistances when heat transfer is directed downward, may be predicted via an understanding of basic heat and mass transfer; however, accurate predictions of thermal resistance values for design and budgeting require experimental techniques. This study has shown the following:

- Samples tested with heat transfer acting downward exhibited substantially (8%–59%) higher thermal resistance values in comparison with the same sample tested with heat transfer acting horizontally.

- Samples lose thermal resistance as sample mean temperature increases. As sample mean temperature increased from 68°F to 95°F, samples with heat transfer acting downward exhibited thermal resistance reductions of 3%–21%. Samples with heat transfer acting horizontally exhibited reductions of 9%–29%.
- Offset girts (IC and UC) help reduce the effect of thermal conduction in the thermal envelope by 5%–13%.
- Installation accuracy can have a substantial effect on thermal resistance values.

Andrew J. Holstein, PhD, is a graduate of the University of Wisconsin–Madison Department of Biological Systems Engineering. David R. Bohnhoff, PhD, PE, is professor emeritus of biological systems engineering at the University of Wisconsin–Madison.

References

ASHRAE. (2017). *2017 ASHRAE Handbook—Fundamentals*. Atlanta, GA: ASHRAE.

Holstein, A. J. (2017). Development of experimental and numerical methods for the evaluation and optimization of building thermal envelopes. PhD diss. Madison, WI: University of Wisconsin–Madison, Department of Biological Systems Engineering.

Holstein, A. J., & Bohnhoff, D. R. (2015). Built for efficiency: A rotatable guarded hot box built for the needs of the post-frame industry. *Frame Building News, 27*(3), 45–49.

Holstein, A. J., Bohnhoff, D. R., & Choi, C. Y. (2018). A computational and experimental study of conjugate heat transfer through composite thermal envelopes in post-frame buildings. *Computers and Electronics in Agriculture, 149*, 139–149.

